NANO LETTERS

Letter

pubs.acs.org/NanoLett

Au Nanostructure-Decorated TiO_2 Nanowires Exhibiting Photoactivity Across Entire UV-visible Region for Photoelectrochemical Water Splitting

Ying-Chih Pu,[†,‡] Gongming Wang,[‡] Kao-Der Chang,[§] Yichuan Ling,[‡] Yin-Kai Lin,[†] Bob C. Fitzmorris,[‡] Chia-Ming Liu,[∥] Xihong Lu,[⊥] Yexiang Tong,[⊥] Jin Z. Zhang,[‡] Yung-Jung Hsu,*[,†] and Yat Li*[,‡]

[†]Department of Materials Science and Engineering, National Chiao Tung University, 1001 University Road, Hsinchu 30010, Taiwan, ROC

[‡]Department of Chemistry and Biochemistry, University of California, Santa Cruz, Santa Cruz, California 95064, United States

[§]Mechanical and Systems Research Laboratories and [∥]Green Energy and Environment Research Laboratories, Industrial Technology Research Institute, 195, Section 4, Chung Hsing Road, Chutung, Hsinchu 31040, Taiwan, ROC

[⊥]KLGHEI of Environment and Energy Chemistry, MOE of the Key Laboratory of Bioinorganic and Synthetic Chemistry, School of Chemistry and Chemical Engineering, Sun Yat-Sen University, Guangzhou 510275, People's Republic of China

Supporting Information

ABSTRACT: Here we demonstrate that the photoactivity of Au-decorated TiO_2 electrodes for photoelectrochemical water oxidation can be effectively enhanced in the entire UV−visible region from 300 to 800 nm by manipulating the shape of the decorated Au nanostructures. The samples were prepared by carefully depositing Au nanoparticles (NPs), Au nanorods (NRs), and a mixture of Au NPs and NRs on the surface of TiO_2 nanowire arrays. As compared with bare TiO_2, Au NP-decorated TiO_2 nanowire electrodes exhibited significantly enhanced photoactivity in both the UV and visible regions. For Au NR-decorated TiO_2 electrodes, the photoactivity enhancement was, however, observed in the visible region only, with the largest photocurrent generation achieved at 710 nm. Significantly, TiO_2 nanowires deposited with a mixture of Au NPs and NRs showed enhanced photoactivity in the entire UV−visible region. Monochromatic incident photon-to-electron conversion efficiency measurements indicated that excitation of surface plasmon resonance of Au is responsible for the enhanced photoactivity of Au nanostructure-decorated TiO_2 nanowires. Photovoltage experiment showed that the enhanced photoactivity of Au NP-decorated TiO_2 in the UV region was attributable to the effective surface passivation of Au NPs. Furthermore, 3D finite-difference time domain simulation was performed to investigate the electrical field amplification at the interface between Au nanostructures and TiO_2 upon SPR excitation. The results suggested that the enhanced photoactivity of Au NP-decorated TiO_2 in the UV region was partially due to the increased optical absorption of TiO_2 associated with SPR electrical field amplification. The current study could provide a new paradigm for designing plasmonic metal/semiconductor composite systems to effectively harvest the entire UV−visible light for solar fuel production.

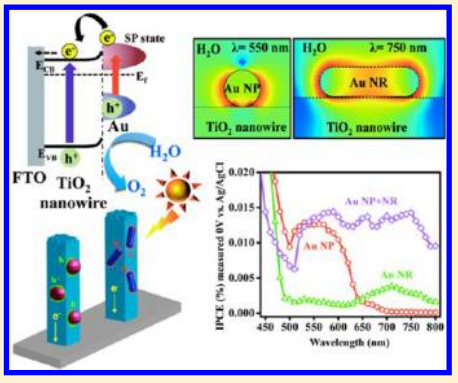

KEYWORDS: *Photoelectrochemical water splitting, plasmonic enhancement, tunable absorption wavelength, solar fuel production, Au, TiO_2*

Titanium dioxide (TiO_2) has been extensively used for photocatalytic and photoelectrochemical generation of solar hydrogen by virtue of its chemical stability, nontoxicity, and relatively low cost.[1−6] However, the large band gap of TiO_2 limits it light absorption to only 5% of solar spectrum.[7−9] TiO_2 has been intentionally doped[10−13] or chemically modified[14−16] to narrow the band gap for harvesting visible light to increase solar-energy utilization. Alternatively, visible-light absorption can also be achieved by coupling TiO_2 to dye molecules[17] or small-band-gap quantum dots.[11,18−21] Recently, a new approach involving metal nanostructures in enhancing the visible-light photoactivity of TiO_2 via plasmonic effect has received much attention.[22−30] In comparison to semiconductor quantum dots that usually suffer from anodic corrosion,[31,32] metal nanoparticles (NPs) have considerably better photostability. Surface plasmon resonance (SPR) is an intrinsic property of metal NPs such as Au, in which the oscillation frequency is highly sensitive to the metal size and shape as well as the dielectric constant of the surrounding environment.[33−36] By acting as an antenna that localizes the optical energy by SPR, plasmonic Au has been suggested to sensitize TiO_2 to light with energy below the band

Received: May 20, 2013
Revised: June 29, 2013
Published: July 30, 2013

   dx.doi.org/10.1021/nl4018385 | *Nano Lett.* 2013, 13, 3817−3823

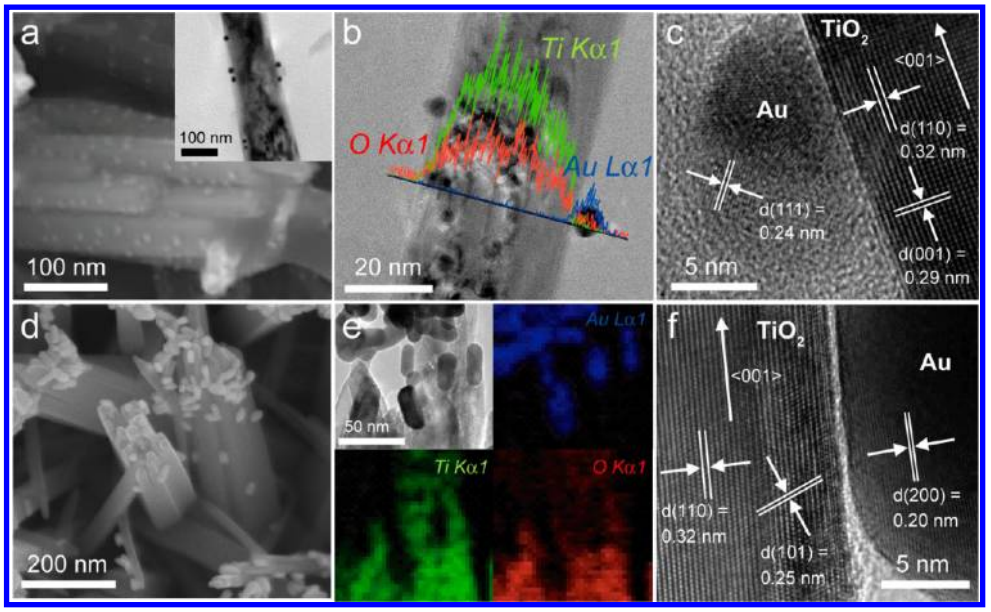

Figure 1. (a) SEM and TEM (inset) images of Au NP-decorated TiO_2 nanowires. (b) EDS linescan profile recorded on an individual Au NP-decorated TiO_2 nanowire. (c) HRTEM image taken at the interface between Au NP and TiO_2 nanowire. (d) SEM images of Au NR-decorated TiO_2 nanowires. (e) TEM image of Au NR-decorated TiO_2 nanowires and the corresponding EDS element-mapping data of Au (blue), Ti (green), and O (red). (f) HRTEM image taken at the interface between Au NR and TiO_2 nanowire.

gap, generating additional charge carriers for water oxidation. Such plasmon-enhanced photoactivity has been reported in several unique Au/TiO_2 composite systems for efficient solar water splitting.[29,30,37−40] For example, Liu et al. reported that the performance of Au NP-deposited TiO_2 films under visible-light illumination for photoelectrochemical water splitting was enhanced 66-fold.[27] This enhancement is due to the SPR-induced electric field amplification near the TiO_2 surface, which increases the photon absorption rate of TiO_2 and thus improves the photoactivity. Besides, Zhang et al. demonstrated that Au nanocrystals assembled with TiO_2-based photonic crystal substrate achieved a high photocurrent density of ∼150 μA/cm^2 under visible-light illumination.[28] These results derived from the matching of the Au SPR wavelength with the photonic band gap of TiO_2, which significantly increased the SPR intensity to boost hot electron injection and therefore enhance the photoactivity.

Previous studies have been primarily focused on the enhancement of photoactivity of TiO_2 in the green region by exploiting the SPR absorption of Au NPs around 550 nm, while the other wavelengths of solar spectrum were not fully utilized. Here we demonstrate that the photoactivity of Au nanostructure-decorated TiO_2 for photoelectrochemical water oxidation can be effectively enhanced in the entire UV−visible region, which was achieved by adopting Au nanostructures with different shapes. The incident photon-to-electron conversion efficiency (IPCE) measurements proved that the enhanced photoactivity of Au nanostructure-decorated TiO_2 in the visible region is strongly correlated with the SPR absorption spectra of the decorating Au. The enhanced photoactivity in UV region can be attributed to the effective passivation of surface states as well as the electric field amplification at the interfaces between TiO_2 and Au upon SPR excitation.

TiO_2 nanowire arrays were synthesized on fluorine-doped tin oxide (FTO) glass substrate by hydrothermal method reported elsewhere (Methods, Supporting Information).[2] The TiO_2 substrate was then immersed in a $HAuCl_4$ solution (pH 4.5) to form $AuCl(OH)_3^-$ complex on TiO_2 surface,[26,41] followed by calcination at 300 °C to grow metallic Au NPs. The scanning electron microscopy (SEM) image of Figure 1a showed that NPs with a typical size of 8 nm were uniformly deposited on the surface of TiO_2 nanowire bundles. Figure 1b displays the energy-dispersive X-ray spectroscopy (EDS) linescan profile recorded on an individual NP-decorated TiO_2 nanowire, which confirmed the composition of Au NPs. The Ti/Au weight ratios of Au NP-decorated TiO_2 nanowires are listed in Table S1 (Supporting Information). In Figure 1c, the high-resolution transmission electron microscopy (HRTEM) image taken at the interface of nanowire and NP regions clearly revealed two distinct sets of lattice fringes, which can be, respectively, assigned to rutile TiO_2 and fcc Au. Note that this sharp interface of TiO_2/Au in Au NP-decorated TiO_2 nanowires is believed to be important for hot electron injection from Au to TiO_2 upon SPR excitation. Moreover, the density of Au NPs can be controlled by varying the time duration of immersing TiO_2 nanowires in $HAuCl_4$ solution. As shown in Figure S1 (Supporting Information), there was no obvious change in the Au particle size as a function of $HAuCl_4$ coating time. SEM-EDS analysis revealed that the Au/Ti weight percentage gradually increased from 0.46 to 2.12% when the Au precursor coating time increased from 1 to 8 h. The as-prepared Au NP-decorated TiO_2 nanowires are denoted as NP-X-TiO_2 (X = number of hours for coating Au precursor).

To obtain Au NR-decorated TiO_2 nanowire sample, we first prepared Au NRs using a seed-growth process.[42] TiO_2 nanowires from hydrothermal synthesis were incubated in mercaptopropionic acid (MPA) solution to create a monolayer on the nanowire surface with the carboxylic acid group attached to TiO_2 and the thiol group exposed outward.[43,44] The surface-functionalized TiO_2 nanowires were then immersed in aqueous suspension of Au NRs for 24 h for attaching Au NRs onto TiO_2 surface. The thus-obtained Au NR-decorated TiO_2 nanowires are denoted as NR-TiO_2. In Figure 1d, the SEM image collected for NR-TiO_2 revealed that Au NRs were successfully

dx.doi.org/10.1021/nl4018385 | Nano Lett. 2013, 13, 3817−3823

loaded on the nanowire surface. The length and width of Au NRs were measured to be about 40 and 15 nm, respectively. Figure 1e shows TEM image of NR-TiO_2 and the corresponding EDS analysis. EDS element-mapping data confirmed that the nanowires are TiO_2 and the rods are Au. In Figure 1f, the lattice-resolved TEM image taken at the interface of nanowire and NR regions showed that the observed interlayer spacings are consistent with the lattice spacings of rutile TiO_2 and fcc Au.[2] Additionally, a small gap was observed between TiO_2 nanowire and Au NR, as expected for the presence of MPA linker molecule.

The photoelectrochemical properties of Au NP- and Au NR-decorated TiO_2 nanowire photoanodes were studied in a three-electrode cell with Ag/AgCl as the reference electrode and a Pt wire as the counter electrode (Methods, Supporting Information). Figure 2a shows a set of linear sweep voltammagrams of bare TiO_2 and Au NP-decorated TiO_2 nanowire (NP-X-TiO_2) electrodes recorded in 1 M NaOH electrolyte in the dark and under white-light illumination (AM 1.5G, 100 mW/cm^2). The dark scans collected in the potential range between −1.0 and +0.5 V versus Ag/AgCl revealed a small background current of ~10^{-8} A/cm^2. Upon illumination with white light, bare TiO_2 and all of the NP-X-TiO_2 electrodes showed pronounced photoresponse. Significantly, NP-X-TiO_2 electrodes exhibited substantially larger photocurrent density than bare TiO_2. Among all of the NP-X-TiO_2 electrodes tested, NP-2-TiO_2 electrode achieved the highest photocurrent density of 1.49 mA/cm^2 at 0 V versus Ag/AgCl, which is almost double the photocurrent density of bare TiO_2 (0.82 mA/cm^2) obtained at the same potential. These results confirmed the positive role of Au NPs in enhancing the photoactivity of TiO_2 electrodes under illumination. To examine the instant photoresponse for the electrodes, the chronoamperomertic $I-t$ curves were collected under chopped light illumination at 0 V versus Ag/AgCl. As shown in Figure 2b (upper panel), the recorded photocurrent densities are consistent with the values obtained from the linear sweep voltammagrams, indicating the photocurrents are stable without photoinduced charging effect.[45] When the Au precursor coating time is more than 2 h, the photocurrent density of NP-X-TiO_2 electrodes decreases gradually with the increase in coating time. This photocurrent depression could be due to two possible reasons. First, the large number of Au NPs grown at the increasing coating time may cover a large portion of the TiO_2 nanowire surface, which retards the access of light to the TiO_2 surface to reduce the photocurrent generation.[46] Second, the high coverage of the Au may reduce the surface area of TiO_2 in direct contact with the electrolyte and thereby hinders the water oxidation performance.

To reveal the plasmonic effect of Au NPs on the photoresponse of TiO_2 electrodes, we collected chronoamperomertic $I-t$ curves for NP-X-TiO_2 electrodes under visible-light illumination by adding a 430 nm long-pass filter to the white-light source (73.3 mW/cm^2 with filter). As shown in Figure 2c, all of the NP-X-TiO_2 electrodes have considerably higher photocurrent density than bare TiO_2. In comparison with bare TiO_2 electrode, the photocurrent density of NP-2-TiO_2 was increased by an order of magnitude under visible-light illumination. Furthermore, the variation of photocurrent densities of NP-X-TiO_2 electrodes under white- and visible-light illumination as a function of Au precursor coating time was found to be similar, implying the same quantitative effect of Au NPs decoration on the enhanced photoactivity of TiO_2 nanowires. This outcome suggests that the enhanced photoactivity of TiO_2 nanowires in UV and visible regions is associated with the SPR effect of deposited Au NPs.

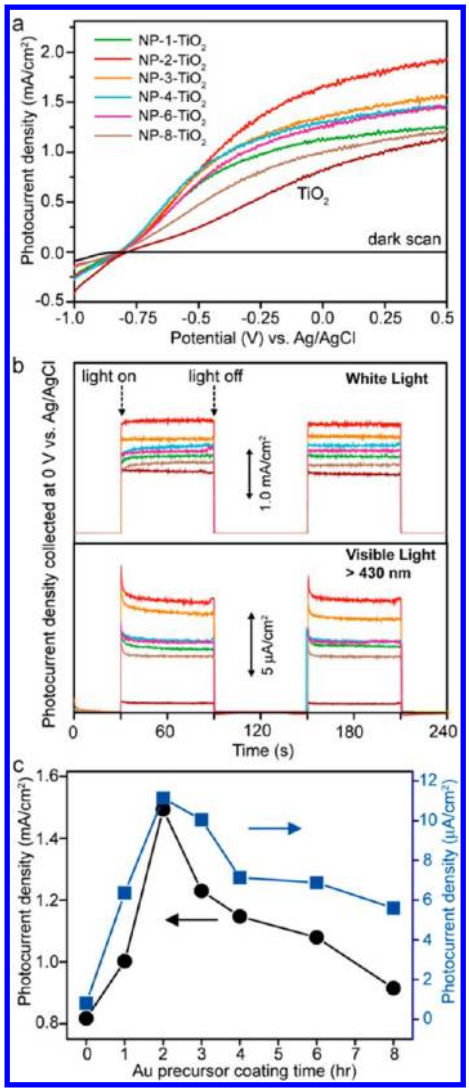

Figure 2. (a) Linear sweep voltammograms of bare TiO_2 and NP-X-TiO_2 electrodes (X = 1, 2, 3, 4, 6, 8) recorded in 1 M aqueous KOH solution in the dark and under white-light illumination (AM 1.5G, 100 mW/cm^2). (b) Chronoamperomertic $I-t$ curves collected at 0 V versus Ag/AgCl for NP-X-TiO_2 electrodes under white-light (AM 1.5G, 100 mW/cm^2) and visible-light (with a 430 nm long pass filter, 73.3 mW/cm^2) illumination. (c) Plot of photocurrent density as a function of Au precursor coating time for NP-X-TiO_2 electrodes under white-light and visible-light illumination.

If the observed photoactivity enhancement of Au NP-decorated TiO_2 nanowires in the visible region was indeed mediated by the SPR excitation, then we should be able to regulate this enhancement to other wavelength regions by manipulating the shape of Au nanostructures, which could shift the SPR absorption wavelength. For example, Au NRs showed SPR that was red-shifted from Au NPs. Figure 3 displays the photoelectrochemical properties of Au NR-decorated TiO_2 nanowire (NR-TiO_2) electrodes. The photocurrent densities of bare TiO_2 and NR-TiO_2 electrodes under white-light illumination are comparable, with the values measured at 0 V versus Ag/AgCl being 0.96 and 0.90 mA/cm^2, respectively. In contrast, under visible light (>430 nm, 73.3 mW/cm^2)

dx.doi.org/10.1021/nl4018385 | Nano Lett. 2013, 13, 3817−3823

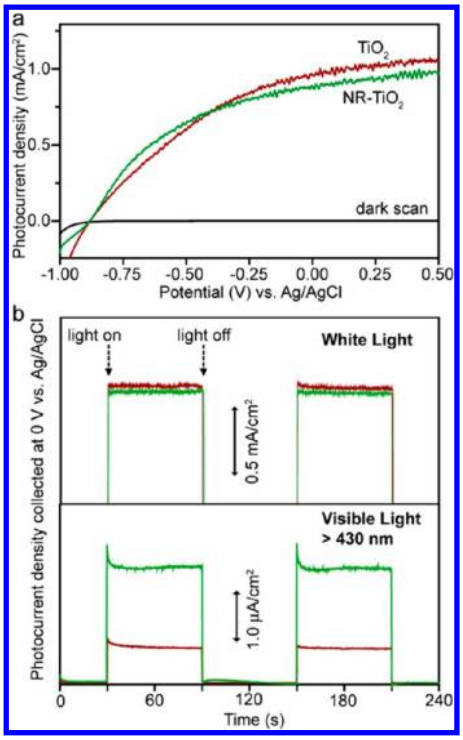

Figure 3. (a) Linear sweep voltammograms of bare TiO_2 and NR-TiO_2 electrodes recorded in 1 M aqueous KOH solution in the dark and under white-light illumination (AM 1.5G, 100 mW/cm^2). (b) Amperometric $I-t$ curves collected at 0 V versus Ag/AgCl for NR-TiO_2 electrodes under white-light (AM 1.5G, 100 mW/cm^2) and visible-light (with a 430 nm long pass filter, 73.3 mW/cm^2) illumination.

illumination the photocurrent density of NR-TiO_2 electrode (2.67 μA/cm^2) is three times higher than that of bare TiO_2 (0.87 μA/cm^2), manifesting the beneficial role of Au NRs in improving the visible-light photoactivity of TiO_2. It is interesting to note that while both Au NPs and Au NRs enhanced the photoactivity of TiO_2 in the visible region, only Au NP-decorated TiO_2 electrode exhibited improved photocurrent under white-light illumination. This discrepancy indicates that the effects of Au NP and Au NR decoration on the enhanced photoactivity of TiO_2 at different wavelengths are essentially different, as will be discussed later.

To further elucidate the role of the decorated Au in enhancing the photoactivity of TiO_2 nanowires, we collected IPCE spectra for bare TiO_2, and Au NP- and Au NR-decorated TiO_2 electrodes at 0 V versus Ag/AgCl. IPCE values at specific wavelengths were calculated based on the following equation:[18]

$$\mathrm{IPCE} = (1240I)/(\lambda J_{\mathrm{light}})$$

where I is the measured photocurrent density, J_{light} is the measured irradiance at a specific wavelength, and λ is the incident light wavelength. The results of IPCE analysis are shown in Figure 4, which revealed several important features. First, for all samples the observed photocurrent is dominated by the photoactivity of TiO_2 in the UV region, reflecting the highly efficient photoconversion of UV light by the TiO_2 nanowires (Figure 4a). Second, the relatively weak photoresponse in the visible region explains the small photocurrent obtained under visible-light illumination. Additionally, only Au NP-decorated TiO_2 electrode showed improved photoactivity in the UV region compared with the bare TiO_2, which is consistent with

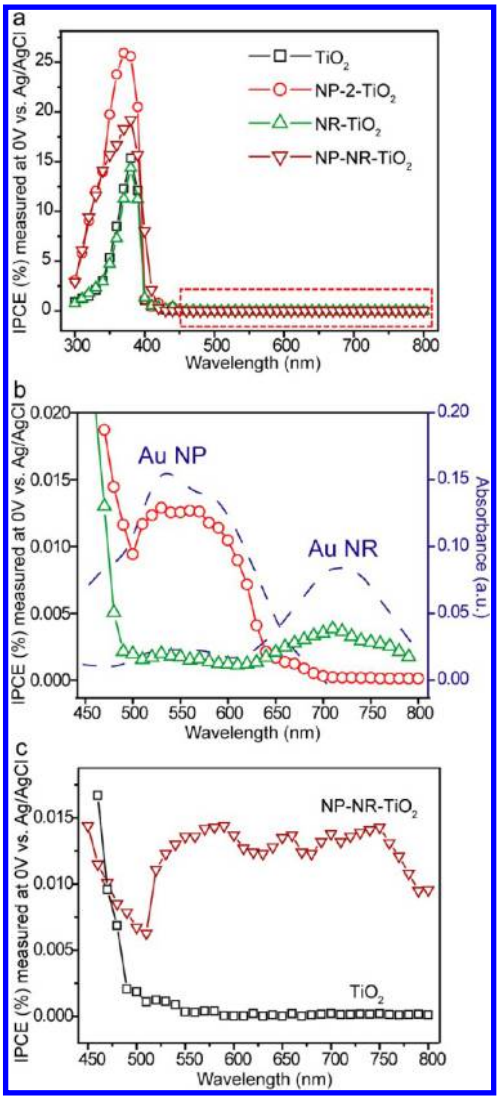

Figure 4. (a) IPCE plots of bare TiO_2 (□), NP-2-TiO_2 (○), NR-TiO_2 (△), and NP-NR-TiO_2 (▽) electrodes collected at 0 V versus Ag/AgCl with the incident wavelength between 300 and 800 nm. (b) Magnified IPCE plots of NP-2-TiO_2 and NR-TiO_2 electrodes in the incident wavelength between 450 and 800 nm, highlighted by the dashed box in panel a. The corresponding absorption spectra of NP-2-TiO_2 and NR-TiO_2 are also included for comparison. (c) Magnified IPCE plots of bare TiO_2 and NP-NR-TiO_2 in the incident wavelength between 450 and 800 nm.

its exclusive photocurrent enhancement observed under white-light illumination. Last but not least, both Au NP- and Au NR-decorated TiO_2 electrodes showed photoactivity enhancement in the visible region when compared with the bare TiO_2. It is noteworthy that Au NP- and Au NR-decorated TiO_2 electrodes have IPCE peaks at different incident light wavelengths, which are well-matched with their corresponding SPR absorption peaks in the visible region (Figure 4b). This SPR wavelength-dependent IPCE feature signifies that excitation of the Au SPR is responsible for the improved visible-light photoactivity of the present Au-decorated TiO_2 nanowires. These results also demonstrated that the plasmon-enhanced photoactivity of TiO_2 is wavelength-tunable by manipulating the shape of the decorating Au nanostructures. In this regard, we further deposit a mixture of Au NPs and NRs on TiO_2 nanowire electrode (denoted as NP-NR-TiO_2), with a goal of expanding its

dx.doi.org/10.1021/nl4018385 | Nano Lett. 2013, 13, 3817−3823

photoactivity. Significantly, as shown in Figure 4c, the NP-NR-TiO_2 electrode exhibited uniformly high IPCE values in the entire visible-light region, which is equivalent to the overlapping wavelength region of NP-2-TiO_2 and NR-TiO_2 electrodes. The photoactivity of NP-NR-TiO_2 in the wavelength between 450 and 600 nm is comparable to that of NP-2-TiO_2. In comparison with the NR-TiO_2 sample, the increased photoactivity of NP-NR-TiO_2 in the wavelength beyond 600 nm was due to the increased loading of Au NRs. Furthermore, we attempted to improve the IPCE performance by increasing the coverage of Au nanostructures. However, the photocurrent of the Au/TiO_2 photoelectrodes decayed when the coverage of the Au nanostructures increased. This was believed to be due to the overloading of Au nanomaterials that not only blocked the light absorption of TiO_2 nanowire but also reduced the interfacial surface area between TiO_2 and the electrolyte, which hindered the transfer of photoexcited holes to the electrolyte for water oxidation.

Several different roles of Au nanostructures in enhancing the photoactivity of semiconductors have been proposed in previous studies, which included the local electric field magnifier,[37,47] the resonant photon scattering center,[22] as well as the hot electrons generator.[28,39] For both electric-field magnification and photon scattering effect, the enhancement of photoactivity should be observed only when the SPR of Au spectrally overlaps with the absorption of semiconductors. For hot electron generation mechanism, it is believed that Au nanostructures serve as a photosensitizer that generates high-energy electrons upon SPR excitation and injects them into the conduction band of the semiconductor. With the efficient supply of hot electrons, semiconductors decorated with Au can exhibit significantly enhanced photoactivity under visible-light illumination.[28,39] To better understand the mechanism of plasmon-enhanced photoactivity in the current system, we investigated the interaction between incident light, TiO_2 nanowires, and the decorated Au. The incident light can interact with Au-decorated TiO_2 nanowire electrodes in three different ways: (1) reflected by the electrode; (2) absorbed by TiO_2 nanowires, and (3) excited surface plasmons of Au.[30] In the first case, incident light will, in general, be partially reflected upon the electrode surface because of the high refractive index of rutile TiO_2 (RI = 2.7).[48,49] The decorated Au can, however, scatter the reflected light back to TiO_2 to improve the overall photon harvesting efficiency. Nevertheless, we suggest that the contribution from light scattering of Au was relatively insignificant considering that the percentage of the decorating Au was rather low (<3.0 wt %). In the second case, the incident photons will be absorbed by TiO_2 nanowires and generate photoexcited electrons and holes. The holes will diffuse to the TiO_2/water interface for water oxidation. Meanwhile, the holes can also recombine with electrons in trap states of TiO_2. Therefore, a high density of surface trap states can negatively affect the photoelectrochemical performance of TiO_2 electrode. We seek to understand the influence of depositing Au on TiO_2 surface on the hole loss associated with trap-state-mediated electron–hole recombination. Photovoltage decay measurement has recently been proven to be a useful method to examine the presence of trap states in photoanode material.[50] We collected photovoltage–time (V–t) spectra for bare TiO_2 and Au NP- and Au NR-decorated TiO_2 electrodes (Figure 5) and calculated the decay lifetime of each V–t profiles by fitting to a biexponential function with two time constants:

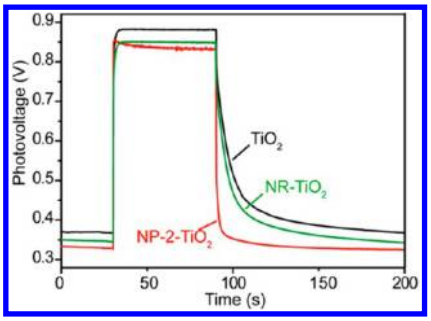

Figure 5. Photovoltage–time spectra collected for bare TiO_2, NP-2-TiO_2, and NR-TiO_2 electrodes.

$$y(t) = A_0 + A_1 e^{-t/\tau_1} + A_2 e^{-t/\tau_2}$$

$$\tau_m = (\tau_1 \tau_2)/(\tau_1 + \tau_2)$$

where τ_m is the harmonic mean of the lifetime and the total half life is $\log(2 \times \tau_m)$. The total half life of bare TiO_2, NP-2-TiO_2, and NR-TiO_2 electrodes was estimated to be 1.94, 0.29, and 1.45 s, respectively. The rapid decay of NP-2-TiO_2 suggests that the deposition of Au NPs could possibly remove surface trap state and reduce the loss of holes via electron–hole recombination. In contrast, the total half life of NR-TiO_2 is just slightly lower than that of bare TiO_2. This could be due to the fact that the presence of surface ligands (MPA) between Au NRs and TiO_2 nanowires limits the ability of Au NRs from effectively passivating surface states, while the growth of Au NPs directly onto the TiO_2 surface maximizes surface passivation. Importantly, the photovoltage decay results support the improved transfer of photoexcited holes to TiO_2 surface for promoting water oxidation upon the deposition of Au NPs. This consequence further infers a conclusion that the enhanced photoactivity of Au NP-decorated TiO_2 electrode in the UV region may be attributed to the passivation of surface trap states.

In the third case, illuminating the decorated Au with visible light can excite surface plasmons that rapidly decay via a series of energy-transfer processes. These processes include resonance photon scattering, plasmon resonance energy transfer (PRET), or production of hot electrons. The resonance photon scattering can be excluded because it normally occurs in large plasmonic nanostructures (over 50 nm in size).[51,52] The effect of PRET describes the interaction of TiO_2 with the SPR-induced electric-field amplification localized nearby at the decorating Au. This interaction promotes the photon absorption of TiO_2 and results in enhanced optical absorption for TiO_2. To assess the extent of electric field amplification upon SPR excitation and its possible contribution to the photoactivity enhancement, we performed the 3-D finite-difference time domain (FDTD) simulation to calculate the spatial distribution of electric-field intensity at the interface of Au and TiO_2 as a function of incident light wavelength. The model for FDTD calculation was depicted in Figure 6a, which contains TiO_2 nanowire domain with width of 50 nm, Au NP with diameter of 10 nm, and Au NR with width and length of 15 and 40 nm. We collected the electric-field intensity versus wavelength data and assumed the incident light traveling along y and z axes. As shown in Figure 6a, the electric-field intensity of Au NP- and Au NR-decorated TiO_2 nanowires was greatly increased in the visible region corresponding to their SPR absorption peaks, qualitatively consistent with the electro-

dx.doi.org/10.1021/nl4018385 | Nano Lett. 2013, 13, 3817–3823

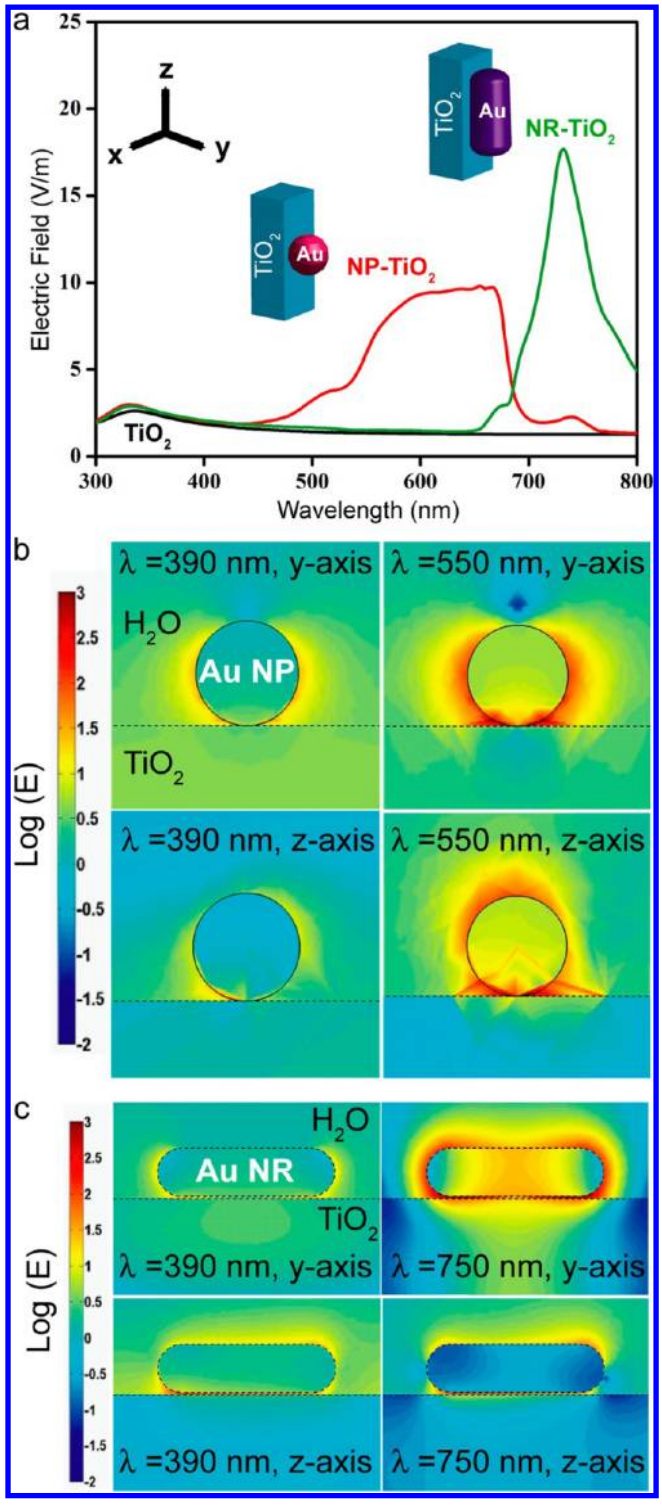

Figure 6. (a) Simulated electric-field intensity plot for bare TiO_2, NP-TiO_2, and NR-TiO_2 nanowires as a function of incident light wavelength. Inset shows schematic model of NP-TiO_2 and NR-TiO_2 nanowires for FDTD simulation. (b,c) Spatial distribution of electric field on the y–z plane for NP-TiO_2 and NR-TiO_2 nanowires. The incident light is along a specific direction (y or z axis).

magnetic field enhancement mechanism typically addressed for plasmonic Au. In addition, a noticeable electric-field increase at the wavelength between 300 to 400 nm was observed for Au NP-decorated TiO_2 sample, which is especially important because it overlapped with the absorption edge of TiO_2. Figures 6b,c further displays the spatial distribution of electric-field intensity at the Au/TiO_2 interface as the monochromatic incident light travels along a specific direction (y or z axes). Under incident light of 390 and 550 nm, the electric-field intensity at the Au NP/TiO_2 interface was increased by two and five times the magnitude, respectively. Likewise, for Au NR-decorated TiO_2 structure, the electric-field intensity at the interface was improved by 15 times the magnitude under incident light of 750 nm. The increase in electric field in the visible region was significant for both Au NP- and Au NR-decorated TiO_2, and it could be accountable for the observed visible light photoactivity enhancement, although there was no spectral overlap between the amplified electric field and the absorption edge of TiO_2. However, it is known that there are defect states within the band gap of TiO_2.[27,53] The low density of these defect states limits the visible-light absorption and thus the photoactivity of TiO_2 in visible region. However, the decoration of Au nanostructures on TiO_2 could lead to substantially enhanced electric field in the visible region and thus visible absorption and photoactivity of TiO_2. On the contrary, the less significant increase in electric field in the UV region for Au NP-decorated TiO_2 sample could lead to its enhanced photoactivity because the amplified electric field in the UV region overlaps with the TiO_2 absorption. This wavelength-dependent FDTD study supports the fact that the enhanced IPCE values of Au NP-decorated TiO_2 nanowires in the UV region are partially due to increased optical absorption of TiO_2 resulting from the PRET effect. Another possible process following the SPR excitation is the generation of energetic hot electrons in Au. It has been suggested that if the hot electrons possess sufficient energy, then they can inject into the conduction band of TiO_2, leaving energetic positive charges at Au that essentially function as holes for water oxidation utilization.[22,54] For the hot electron injection mechanism, the photoactivity enhancement can occur at energy well below the band gap of TiO_2. Therefore, the enhanced photoactivity of Au NP- and Au NR-decorated TiO_2 nanowires in the visible region is mainly ascribed to the hot electron generation upon SPR excitation.

In summary, we demonstrated that the photoactivity of Au nanostructure-decorated TiO_2 nanowire electrodes for photoelectrochemical water oxidation can be effectively enhanced in the entire UV–visible region by adopting different shapes of the decorating Au nanostructures. The results of IPCE measurement, photovoltage experiment, and FDTD simulation suggest that the enhanced photoactivity of Au NP-decorated TiO_2 nanowires in the UV region is due to effective surface passivation as well as electric-field amplification effect, while the photoactivity enhancement in the visible region for Au nanostructure-decorated TiO_2 samples is mainly caused by the electrical field amplification effect and hot electron generation upon SPR excitation. The ability to tune and expand the photoactivity of Au-decorated TiO_2 electrodes from the UV to the visible region makes it possible to design composite plasmonic metal/semiconductor photoelectrodes to more effectively utilize the solar spectrum.

■ ASSOCIATED CONTENT

Supporting Information

Synthetic and analytical methods and SEM images. This material is available free of charge via the Internet at http://pubs.acs.org.

dx.doi.org/10.1021/nl4018385 | Nano Lett. 2013, 13, 3817–3823

AUTHOR INFORMATION

Corresponding Author

*E-mail: yhsu@cc.nctu.edu.tw (Y.-J.H.); yli@chemistry.ucsc.edu (Y.L.).

Notes

The authors declare no competing financial interest.

ACKNOWLEDGMENTS

Y.J.H. acknowledges the financial support from the National Science Council of Taiwan (NSC-100-2113-M-009-004, NSC-101-2113-M-009-018, and NSC-101-3113-P-009-005). Y.L. acknowledges the financial support from United States NSF (DMR-0847786). J.Z.Z thanks the BES Division of the U.S. DOE (DEFG02-ER46232) for financial support. Y.C.P. thanks the National Science Council of Taiwan for sponsoring the Graduate Students Study Abroad Program (NSC-102-2917-I-009-042). We thank C. Funatogawa and Prof. O. Einarsdottir for providing the centrifuge facility.

REFERENCES

(1) Fujishima, A.; Honda, K. *Nature* **1972**, *238*, 37−38.
(2) Wang, G.; Wang, H.; Ling, Y.; Tang, Y.; Yang, X.; Fitzmorris, R. C.; Wang, C.; Zhang, J. Z.; Li, Y. *Nano Lett.* **2011**, *11*, 3026−3033.
(3) Cho, I. S.; Chen, Z.; Forman, A. J.; Kim, D. R.; Rao, P. M.; Jaramillo, T. F.; Zheng, X. *Nano Lett.* **2011**, *11*, 4978−4984.
(4) Mohapatra, S. K.; Misra, M.; Mahajan, V. K.; Raja, K. S. *J. Phys. Chem. C* **2007**, *111*, 8677−8685.
(5) Noh, S. Y.; Sun, K.; Choi, C.; Niu, M.; Yang, M.; Xu, K.; Jin, S.; Wang, D. *Nano Energy* **2013**, *2*, 351−360.
(6) Lin, Y.; Yuan, G.; Liu, R.; Zhou, S.; Sheehan, S. W.; Wang, D. *Chem. Phys. Lett.* **2011**, *507*, 209−215.
(7) Kruse, O.; Rupprecht, J.; Mussgnug, J. H.; Dismukes, G. C.; Hankamer, B. *Photochem. Photobiol. Sci.* **2005**, *4*, 957−969.
(8) Malato, S.; Fernández-Ibáñez, P.; Maldonado, M. I.; Blanco, J.; Gernjak, W. *Catal. Today* **2009**, *147*, 1−59.
(9) Leary, R.; Westwood, A. *Carbon* **2011**, *49*, 741−772.
(10) López-Luke, T.; Wolcott, A.; Xu, L.-p.; Chen, S.; Wen, Z.; Li, J.; Rosa, E. D. L.; Zhang, J. Z. *J. Phys. Chem. C* **2008**, *112*, 1282−1292.
(11) Liu, L.; Hensel, J.; Fitzmorris, R. C.; Li, Y.; Zhang, J. Z. *J. Phys. Chem. Lett.* **2010**, *1*, 155−160.
(12) Park, J. H.; Kim, S.; Bard, A. J. *Nano Lett.* **2006**, *1*, 24−28.
(13) Xu, M.; Da, P.; Wu, H.; Zhao, D.; Zheng, G. *Nano Lett.* **2012**, *12*, 1503−1508.
(14) Chen, X.; Liu, L.; Yu, P. Y.; Mao, S. S. *Science* **2011**, *331*, 746−750.
(15) Khan, S. U. M.; Al-Shahry, M.; Ingler, W. B., Jr. *Science* **2002**, *297*, 2243−2245.
(16) Qiu, J.; Qiu, Y.; Yan, K.; Zhong, M.; Mu, C.; Yan, H.; Yang, S. *Nanoscale* **2013**, *5*, 3245−3248.
(17) Youngblood, W. J.; Lee, S.-H. A.; Kobayashi, Y.; Hernandez-Pagan, E. A.; Hoertz, P. G.; Moore, T. A.; Moore, A. L.; Gust, D.; Mallouk, T. E. *J. Am. Chem. Soc.* **2009**, *131*, 926−927.
(18) Wang, H.; Wang, G.; Ling, Y.; Lepert, M.; Wang, C.; Zhang, J. Z.; Li, Y. *Nanoscale* **2012**, *4*, 1463−1466.
(19) Hensel, J.; Wang, G.; Li, Y.; Zhang, J. Z. *Nano Lett.* **2010**, *10*, 478−483.
(20) Cheng, C.; Karuturi, S. K.; Liu, L.; Liu, J.; Li, H.; Su, L. T.; Tok, A. I.; Fan, H. J. *Small* **2012**, *8*, 37−42.
(21) Selinsky, R. S.; Ding, Q.; Faber, M. S.; Wright, J. C.; Jin, S. *Chem. Soc. Rev.* **2013**, *42*, 2963−2985.
(22) Linic, S.; Christopher, P.; Ingram, D. B. *Nat. Mater.* **2011**, *10*, 911−921.
(23) Wang, H.; You, T.; Shi, W.; Li, J.; Guo, L. *J. Phys. Chem. C* **2012**, *116*, 6490−6494.
(24) Wu, F.; Hu, X.; Fan, J.; Liu, E.; Sun, T.; Kang, L.; Hou, W.; Zhu, C.; Liu, H. *Plasmonics* **2012**, 1−8.
(25) Seh, Z. W.; Liu, S.; Low, M.; Zhang, S. Y.; Liu, Z.; Mlayah, A.; Han, M. Y. *Adv. Mater.* **2012**, *24*, 2310−2314.
(26) Silva, C. G.; Juárez, R.; Marino, T.; Molinari, R.; García, H. *J. Am. Chem. Soc.* **2011**, *133*, 595−602.
(27) Liu, Z.; Hou, W.; Pavaskar, P.; Aykol, M.; Cronin, S. B. *Nano Lett.* **2011**, *11*, 1111−1116.
(28) Zhang, Z.; Zhang, L.; Hedhili, M. N.; Zhang, H.; Wang, P. *Nano Lett.* **2013**, *13*, 14−20.
(29) Hou, W.; Cronin, S. B. *Adv. Funct. Mater.* **2012**, *23*, 1612−1619.
(30) Warren, S. C.; Thimsen, E. *Energy Environ. Sci* **2012**, *5*, 5133−5146.
(31) Chen, H. M.; Chen, C. K.; Chang, Y. C.; Tsai, C. W.; Liu, R. S.; Hu, S. F.; Chang, W. S.; Chen, K. H. *Angew. Chem., Int. Ed.* **2010**, *49*, 5966−5969.
(32) Lee, Y.-L.; Chi, C.-F.; Liau, S.-Y. *Chem. Mater.* **2010**, *22*, 922−927.
(33) Jain, P. K.; El-Sayed, M. A. *Nano Lett.* **2008**, *8*, 4347−4352.
(34) Kelly, K. L.; Coronado, E.; Zhao, L. L.; Schatz, G. C. *J. Phys. Chem. B* **2003**, *107*, 668−677.
(35) Chou, C.-H.; Chen, C.-D.; Wang, C. R. C. *J. Phys. Chem. B* **2005**, *109*, 11135−11138.
(36) Li, C.; Shuford, K. L.; Chen, M.; Lee, E. J.; Cho, S. O. *ACS Nano* **2008**, *2*, 1760−1769.
(37) Gao, H.; Liu, C.; Jeong, H. E.; Yang, P. *ACS Nano* **2012**, *6*, 234−240.
(38) Lee, J.; Mubeen, S.; Ji, X.; Stucky, G. D.; Moskovits, M. *Nano Lett.* **2012**, *12*, 5014−5019.
(39) Chen, H. M.; Chen, C. K.; Chen, C.-J.; Cheng, L.-C.; Wu, P. C.; Cheng, B. H.; Ho, Y. Z.; Tseng, M. L.; Hsu, Y.-Y.; Chan, T.-S.; Lee, J.-F.; Liu, R.-S.; Tsai, D. P. *ACS Nano* **2012**, *6*, 7362−7372.
(40) Thimsen, E.; Formal, F. L.; Grätzel, M.; Warren, S. C. *Nano Lett.* **2011**, *11*, 35−43.
(41) Pu, Y.-C.; Chen, Y.-C.; Hsu, Y.-J. *Appl. Catal., B* **2010**, *97*, 389−397.
(42) Sau, T. K.; Murphy, C. J. *Langmuir* **2004**, *20*, 6414−6420.
(43) Zhang, Y. X.; Huang, M.; Hao, X. D.; Dong, M.; Li, X. L.; Huang, J. M. *Nanoscale Res. Lett.* **2012**, *7*, 1−5.
(44) Choi, H.; Santra, P. K.; Kamat, P. V. *ACS Nano* **2012**, *6*, 5718−5726.
(45) Wang, G.; Ling, Y.; Lu, X.; Zhai, T.; Qian, F.; Tong, Y.; Li, Y. *Nanoscale* **2013**, *5*, 4129−4133.
(46) Lu, W.; Gao, S.; Wang, J. *J. Phys. Chem. C* **2008**, *112*, 16792−16800.
(47) Thomann, I.; Pinaud, B. A.; Chen, Z.; Clemens, B. M.; Jaramillo, T. F.; Brongersma, M. L. *Nano Lett.* **2011**, *11*, 3440−3446.
(48) Liu, X.; Zhou, W.; Yin, Z.; Hao, X.; Wu, Y.; Xu, X. *J. Mater. Chem.* **2012**, *22*, 3916−3021.
(49) Liu, J.-g.; Nakamura, Y.; Ogura, T.; Shibasaki, Y.; Ando, S.; Ueda, M. *Chem. Mater.* **2008**, *20*, 273−281.
(50) Mukherjee, B.; Wilson, W.; Subramanian, V. R. *Nanoscale* **2013**, *5*, 269−274.
(51) Evanoff, D. D., Jr.; Chumanov, G. *ChemPhysChem* **2005**, *6*, 1221−1231.
(52) Burda, C.; Chen, X.; Narayanan, R.; El-Sayed, M. A. *Chem. Rev.* **2005**, *105*, 1025−1102.
(53) Wang, G.; Ling, Y.; Li, Y. *Nanoscale* **2012**, *4*, 6682−6691.
(54) Tian, Y.; Tatsuma, T. *J. Am. Chem. Soc.* **2005**, *127*, 7632−7637.